Volume 59
Number 69
7 September 2023
Pages 10321–10454

ChemComm

Chemical Communications

rsc.li/chemcomm

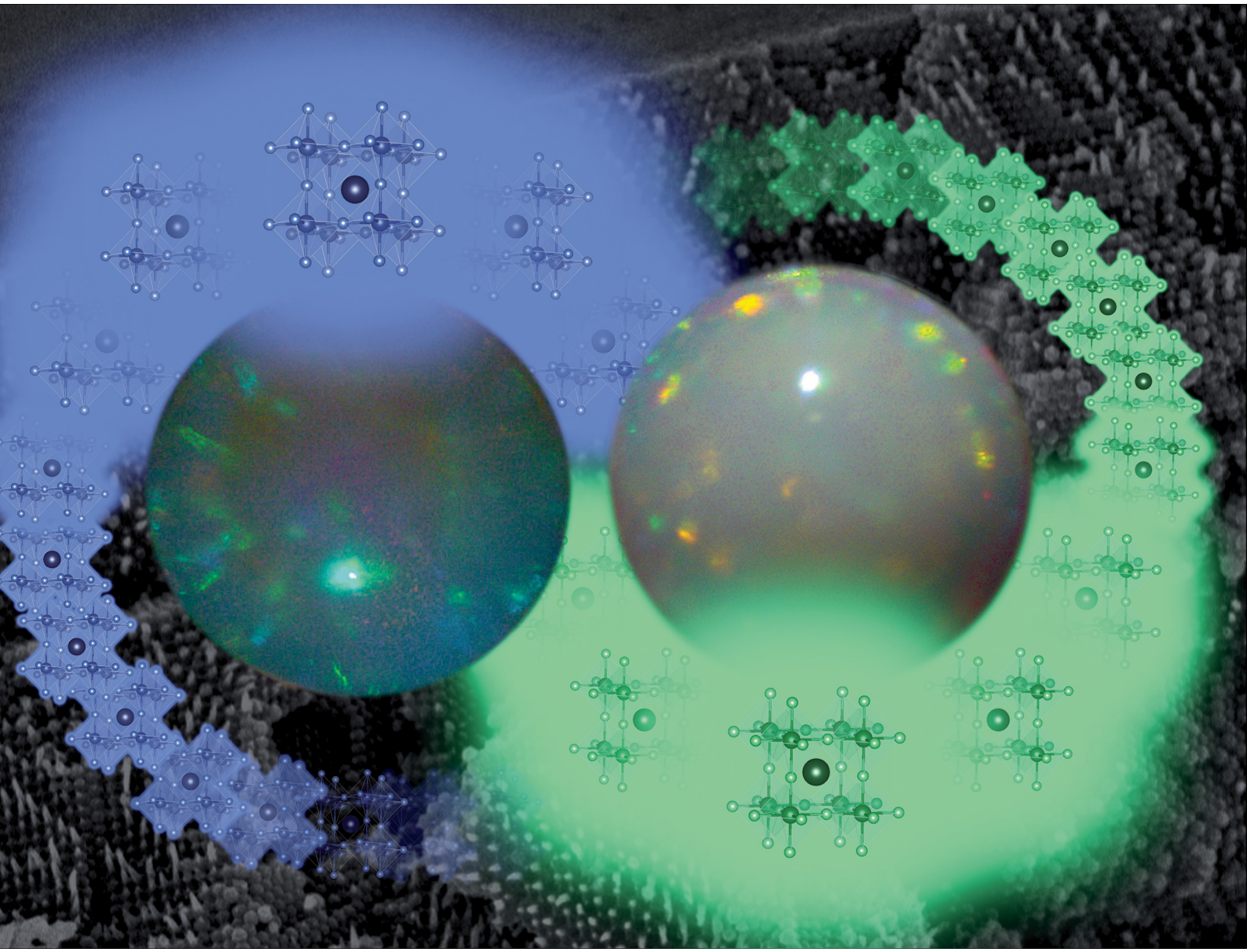

ISSN 1359-7345

ROYAL SOCIETY OF CHEMISTRY

COMMUNICATION

Marek B. Majewski *et al.*

Photonic enhancement in photoluminescent metal halide perovskite–photonic crystal bead hybrids

ChemComm

COMMUNICATION

View Article Online
View Journal | View Issue

Cite this: *Chem. Commun.*, 2023, **59**, 10380

Received 21st June 2023,
Accepted 31st July 2023

DOI: 10.1039/d3cc02962j

rsc.li/chemcomm

Photonic enhancement in photoluminescent metal halide perovskite–photonic crystal bead hybrids†

Victoria Lapointe,[a] Christian J. Imperiale,[b] Sollavi Chengadu,[a] Cristina M. Pomilio,[a] Meera Ganesh,[a] Stephane Kéna-Cohen[b] and Marek B. Majewski *[a]

We report two photonic crystal-perovskite nanocrystal microbead hybrids with photoluminescence matching that of the parent nanocrystals but with increased photoluminescence quantum yields. Time-resolved photoluminescence spectroscopy quantifies the radiative enhancement afforded by the photonic environment of the microbeads. The reported hybrids also demonstrate markedly better resistance to degradation in water over 30 days of immersion.

Metal halide perovskite nanocrystals (PNCs) are promising materials for many applications like light-emitting diodes,[1] photodetectors,[2,3] and photocatalysts.[4,5] The general formula for PNCs is ABX_3 where A is a monovalent cation, B is a divalent metal cation, and X is a halide anion.[6,7] Most of the optoelectronic properties originate from the B-site metal and halide orbitals which enable a tunable bandgap and modulate the corresponding photoluminescence.[5,6] Purely inorganic metal halide PNCs exhibit higher photoluminescence quantum yields, and greater chemical and physical stability over hybrid perovskites incorporating organic cations, however they are not indefinitely stable.[1,8] Their moisture sensitivity leads to long-term ambient instability, and a reduction in charge carrier recombination lifetimes limiting their commercial viability.[1,8,9]

Photonic crystals (PCs) are periodic dielectric environments able to manipulate the propagation of light in one, two, or many directions. While artificial crystals are commonly fabricated for photonic applications,[10–13] PCs are also found in nature in opals and butterfly wings.[14–18] The shape, periodicity and refractive index of the elemental PC building block and lattice structure determine the dispersion relation of the photon modes that can propagate within the PC. In some cases, photonic stopbands can form for certain frequencies of light, within which propagation cannot occur. These are analogous to the formation of electronic bandgaps in solid-state systems and light incident on the PC within the stopband will be reflected.[18] In addition, the vanishing group velocity that occurs at band edges leads to slow light propagation and maxima in the photonic density of states that can be used to increase the spontaneous emission rate of nearby emitters. The ability of PCs to manipulate light propagation has been used to enhance light-harvesting efficiencies for photocatalysis,[19–22] optoelectronic devices[22–24] and photoluminescent sensors.[15,25,26]

Considering the tunable bandgaps and band structure of PNCs and PCs, respectively, their combination as a hybrid system is a testbed for modifying optoelectronic properties by relating the photoluminescence to the photonic band structure formed by the PC. The hybrid system can also increase the physical stability of PNCs through encapsulation in inert and hydrophobic PC materials.[14,16] Intrigued by the possibility of optoelectronic effects arising from these types of hybrids that are still underexplored, we report a PC⊂PNC microbead hybrid system composed of polystyrene spheres (190 and 370 nm in diameter, referred to as 190PC and 370PC, respectively) and metal halide PNCs ($CsPbBr_3$ and $CsPbBr_{1.5}Cl_{1.5}$). The PNCs are prepared independently of the PCs, and the hybrids are prepared using a simple vacuum-drying technique. We discover that these photoluminescent PC⊂PNC microbead hybrid systems exhibit photoluminescence quantum yields (PLQY) that are up to 3× greater than the starting PNC colloid. We further clarify our observations of increased PLQY using time-resolved photoluminescence (TRPL) spectroscopy and find radiative rate enhancements of 28% ($CsPbBr_3$) and 100% ($CsPbBr_{1.5}Cl_{1.5}$) from the PC environment. Finally, these hybrid systems exhibit remarkable resistance to water for up to 30 days, a crucial improvement towards longer-term applications.

While the present synthesis of PC microbeads is based on previous reports, a degree of optimization was necessary to generate spherical beads of sufficient optical quality for follow-

[a] *Department of Chemistry and Biochemistry and Centre for NanoScience Research Concordia University, 7141 Sherbrooke Street West, Montreal, Quebec H4B 1R6, Canada. E-mail: marek.majewski@concordia.ca*

[b] *Department of Engineering Physics, Polytechnique Montréal, Montréal, Quebec, Canada*

† Electronic supplementary information (ESI) available. See DOI: https://doi.org/10.1039/d3cc02962j

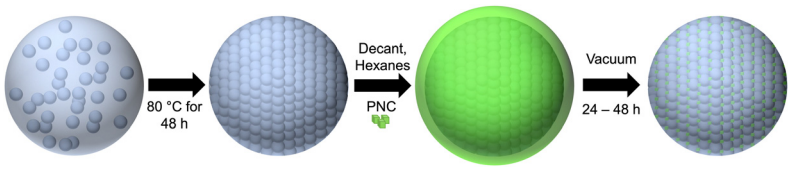

Scheme 1 Summary of synthetic procedures for preparing PC⊂PNC microbead hybrids.

on studies (Scheme 1).[6,18] Preparation of metal halide PNCs followed a typical hot-injection synthesis as reported by Protesescu *et al.*[7] (see ESI† for experimental details). In this work we opted for post-synthetic addition of the PNCs to PC microbeads to reduce any structural alteration to the individual PCs that may in turn affect the stability and optical properties of the hybrid system. Here, vacuum-drying of a PNC solution in the presence of preassembled PC microspheres yielded a hybrid material that did not lose any coloration or exhibit any apparent surface film formation upon rinsing with hexane, providing evidence that PNCs had been drawn into the voids formed within the PC structure.

A careful analysis of the optical properties of PNCs and PCs individually determined which PNC would be a most suitable match to the different PC microbeads (*i.e.*, to approach the photonic stopband of the PC with the photoluminescence maximum of the PNCs). PC microbeads were analyzed by collecting reflectance spectra where a photonic stopband of 2.24 eV (554 nm) was determined for the 370PC microbeads while for the 190PC microbeads, a photonic stopband of 2.74 eV (452 nm) was calculated (Fig. 1A and Fig. S1, ESI†). These photonic stopbands closely match those reported by Chen *et al.*[18] Qualitatively, the calculated stopband is also observed in the optical micrographs under white light illumination (Fig. S2A, B and Fig. S3, ESI†). After evaluating the absorbance and photoluminescence spectra of several $CsPbX_3$ PNCs, two were found to correlate best with the PC photonic stopbands. $CsPbBr_3$ PNCs dispersed in hexanes yielded a bandgap energy (E_g) of 2.52 eV (492 nm), a photoluminescence maximum (λ_{em}) = 2.48 eV (500 nm) with a full width at half maximum (FWHM) value of 150 meV (30 nm) and a PLQY of 66 ± 5% when excited at 365 nm (Fig. S4 and S5, ESI†). The relatively narrow FWHM indicates that the PNC sample is monodisperse while the PLQY value falls within the expected literature value of 50–80%.[1] $CsPbBr_{1.5}Cl_{1.5}$ PNCs (here the stoichiometry represents the stoichiometry of the reactants, not that of the final product) dispersed in hexanes yielded a E_g of 2.86 eV (433 nm) and λ_{em} = 2.81 eV (441 nm) with a FWHM of 170 meV (26 nm) and PLQY of 7 ± 3% when excited at 365 nm (Fig. S6, ESI†). The low PLQY of $CsPbBr_{1.5}Cl_{1.5}$ PNCs is expected as violet-blue emitting PNCs suffer from higher Cl^- vacancies and deeper trap sites.[5,27] From the calculated photonic stopbands, it was determined that $CsPbBr_3$ PNCs may be an appropriate match for 370PC microbeads and the $CsPbBr_{1.5}Cl_{1.5}$ PNCs for 190PC microbeads since the photoluminescence maxima in both cases are marginally higher in energy than the photonic stopbands of these microbeads (ΔE = 0.24 eV and 0.07 eV, respectively) ensuring PNC energies correspond near a band edge of the PC, for which the photonic density of states has a maximum.

Incorporation of the PNCs into PC microbeads through vacuum-drying yielded hybrids: 370PC⊂$CsPbBr_3$ and 190PC⊂$CsPbBr_{1.5}Cl_{1.5}$. The reflectance spectra demonstrate both the photonic stopband of the PC microbeads and the bandgap energy derived from the PNCs simultaneously (Fig. 1B). Qualitatively, no significant changes were observed in the optical micrographs of the beads as their reflective and opalescent properties were unaffected by the incorporation of PNCs (Fig. 2A and B). The PC⊂PNC microbead hybrids exhibit photoluminescence spectra analogous to those of the PNC colloids (Fig. 1B). The 370PC⊂$CsPbBr_3$ hybrid has λ_{em} = 2.46 eV (502 nm), a FWHM of 94 meV (20 nm) and a PLQY of 74 ± 10% while the 190PC⊂$CsPbBr_{1.5}Cl_{1.5}$ hybrid has λ_{em} = 2.81 eV (442 nm), a FWHM of 115 meV (18 nm) and a PLQY of 21 ± 7%. These results represent a slightly red-shifted λ_{em} (max. 20 meV/2 nm) and a small increase in FWHM values (max. 55 meV/8 nm) often explained by a phase transition and/or a decrease in monodispersity.[7,27,28] Powder X-ray diffraction confirms incorporation of PNCs within the PC (Fig. S7 and S8, ESI†). This was further confirmed by scanning electron microscopy-energy dispersive spectroscopy (SEM-EDS) mapping (Fig. S9–S12, ESI†) where infiltration of the expected PNC elements into the PC

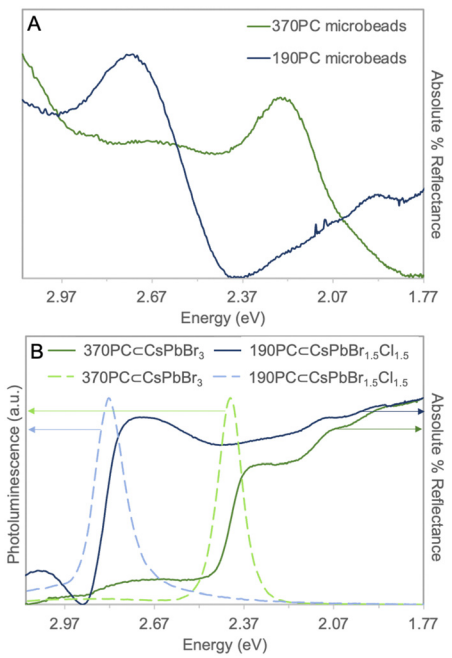

Fig. 1 (A) Absolute % reflectance of 370PC and 190PC microbeads and (B) normalized optical data for 370PC⊂$CsPbBr_3$ and 190PC⊂$CsPbBr_{1.5}Cl_{1.5}$ hybrids (λ_{ex} = 365 nm).

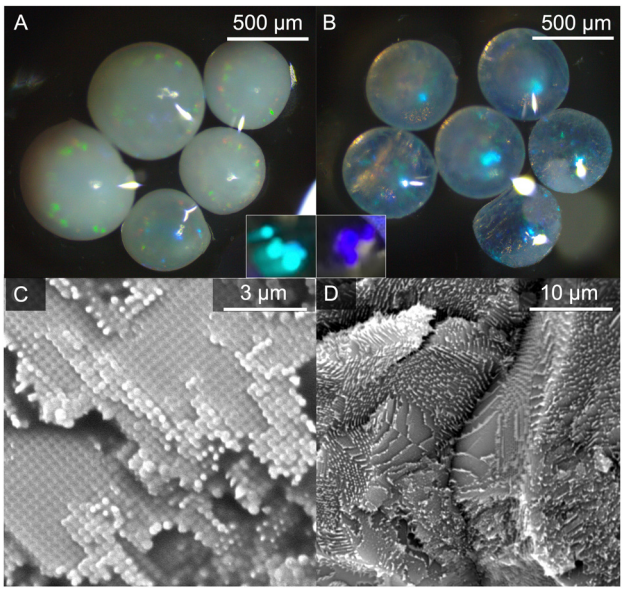

Fig. 2 Optical micrographs of (A) 370PC⊂$CsPbBr_3$ and (B) 190PC⊂$CsPbCl_{1.5}Br_{1.5}$ microbead hybrids exposed to light from above in silicone oil with insets of hybrids illuminated with λ_{ex} = 365 nm. SEM of (C) 370PC⊂$CsPbBr_3$ and (D) 190PC⊂$CsPbCl_{1.5}Br_{1.5}$.

structure is apparent. The SEM micrographs (Fig. 3D–F) also indicate that this technique does not affect the structure of the polystyrene PCs.

The highlight of the present results is the increase in PLQY of the hybrids (*ca.* 8%) as compared to the PNC colloids (PLQY = 74%). Such increases in PLQY after PC⊂PNC microbead incorporation have yet to be reported. We hypothesize that the close match between the photoluminescence maxima of the PNCs and the edge the photonic stopband gives rise to a favorable photonic environment that promotes increased radiative decay rates in the embedded PNCs, commonly referred to as Purcell enhancement.[27] This phenomenon can be understood as an increase in the photonic density of final states for the radiative transition, owing to the large group velocities that occur at the edge of the bandgap.[28,29] Consequently, the enhanced radiative rate outcompetes the intrinsic non-radiative decay processes within the PNCs themselves, giving rise to brighter emission.

To clarify the underlying decay processes governing this behaviour, we used time-resolved photoluminescence (TRPL) spectroscopy to study the excited-state dynamics of these hybrid materials. Neat $CsPbBr_3$ PNC films exhibit excitation-density-dependent PL dynamics (Fig. S13, ESI†), proceeding from nearly mono-exponential to highly multi-exponential decays characteristic of non-geminate carrier recombination processes at higher excitation densities.[30,31] Thus, we focus upon the low-fluence regime in this work to minimize the impact of intensity-dependent decay processes in our observations. Comparing the PL dynamics of the neat $CsPbBr_3$ film to those measured from PNCs integrated within our hybrid systems, an increase in the decay rate of those PNCs within the photonic environment was observed (Fig. 3A). While the average lifetime of the neat $CsPbBr_3$ film is 2.1 ns (A = 0.5, τ_1 = 0.6 ns, τ_2 = 2.6 ns), the amplitude-weighted average lifetime of the $CsPbBr_3$ PNCs within the hybrid is 1.7 ns (A = 0.6, τ_1 = 0.2 ns, τ_2 = 2.0 ns). Intriguingly, the PC-integrated PNCs possess early time (t < 1 ns) dynamics accounting for 60% of the prepared photoexcitations, before exhibiting later-time dynamics more closely comparable to the neat PNC film (t > 1 ns). This observation provides evidence that a majority of the PNCs within the microbeads experience some radiative enhancement owing to the Purcell effect. In fact, approximating the theoretical PLQY of these PC-integrated PNCs using the amplitude-weighted decay components of the biexponential fit predicts a 28% increase in the PLQY (67% → 86%) strictly from radiative enhancement (assuming identical non-radiative decay rates; see ESI† for sample calculations). This is slightly greater than, though comparable to, the increase we measure from direct PLQY measurements (PLQY = 74%). Indeed, since an increase in the measured steady-state PLQY (*vide supra*) is observed, we consider this to be a conservative estimate of the achievable enhancement factor within the photonic microbeads, concomitant with minor alterations to underlying non-radiative decay processes within the PNC assemblies.

Likewise, mixed-halide PNCs ($CsPbCl_{1.5}Br_{1.5}$) demonstrate similar PL decay dynamics both before and after integration within the photonic crystal structure (Fig. 3B). Here, a greater change in the fitted lifetime is observed, stemming from both an increase in rate and amplitude of the early-time PL decay component. The average lifetime of the neat PNC film is 2.9 ns (A = 0.4, τ_1 = 0.5 ns, τ_2 = 3.1 ns), while the average lifetime of the PNCs within the hybrid is 2.0 ns (A = 0.6, τ_1 = 0.3 ns, τ_2 = 2.4 ns).

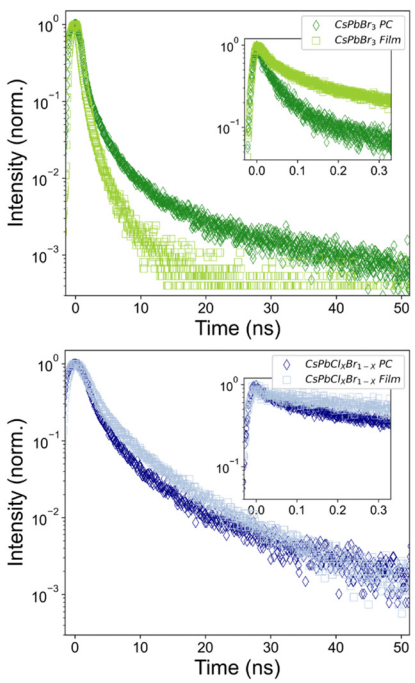

Fig. 3 Time-resolved photoluminescence (TRPL) dynamics of neat PNC films and PC⊂PNCs. PL decay traces of: (A) $CsPbBr_3$ NCs (λ_{ex} = 390 nm). (B) $CsPbCl_{1.5}Br_{1.5}$ NCs (λ_{ex} = 350 nm).

Applying the same competing rate analysis as above, we estimate a 100% (two-fold) theoretical enhancement in the PLQY (7% → 14%)—an underestimate of the three-fold-enhanced PLQY of 21% that we report above. Taken together, these TRPL and PLQY data point toward an enhancement in the radiative decay channels PNCs within our PC⊂PNC hybrids.

Once a reproducible synthetic method was established for the PC⊂PNC hybrids, a water stability test was conducted as a means of understanding how their incorporation affects their physical and optical properties.

As colloids dropped into water, $CsPbBr_3$ PNCs and $CsPbBr_{1.5}Cl_{1.5}$ PNCs no longer exhibit photoluminescence after *ca.* 225 seconds and 75 seconds, respectively (Fig. S14A, ESI†). Conversely, PC⊂PNC hybrids still demonstrate photoluminescence after 30 days of being immersed in water (albeit decreasing in intensity; Fig. S14B, C and S15, ESI†) and show negligible changes in the PC⊂PNC reflectance, opalescence, and structure (Fig. S16–S20, ESI†). Both microbead hybrid systems exhibit a similar trend of red-shifting λ_{em} and increasing FWHM values. These results correspond to the PNCs decomposing from their smaller, photoluminescent morphology, to their bulk, non-photoluminescence counterpart.[28] Although these results demonstrate the PC⊂PNC hybrids are not indefinitely stable, they have allowed for a marked increase in stability in water *versus* PNC colloids—implying an even greater tolerance for ambient moisture. This higher resistance to decomposition may be due to electrostatic stabilization between the positively charged polystyrene matrix and the negatively charged surface of PNCs.[8] This over-30-day stability of PC⊂PNC hybrids in water shows great promise for optoelectronic applications where the long-term stability of PNC assemblies is a concern.

In conclusion, PC–PNC hybrid systems were synthesized using a simple vacuum drying technique which allowed for the PC and PNC optical properties to be simultaneously observed without deteriorating either material. The incorporated material showed increased PLQY compared to the PNC-only counterparts, arising from the photonic environment attributed to the Purcell effect and confirmed by TRPL measurements. Additionally, the improved long-term water stability demonstrates the practical improvements provided by our approach motivating the further development of such hybrids within solar energy conversion and light emitting devices.

V. L., S. C., C. P., and M. G. carried out synthetic experimental work and characterization. C. J. I. carried out TRPL and supplemental PLQY measurements. The manuscript was written by V. L., C. J. I., S. K. C. and M. B. M. The authors thank Natural Sciences and Engineering Research Council of Canada (NSERC) [M. B. M. funding: RGPIN-2018-04391], Fonds de Recherche du Québec – Nature et technologies (FRQNT), Canada Research Chairs Program (S. K. C.), and Quebec Centre for Advanced Materials (QCAM) for financial support. V. L. thanks NSERC and FRQNT for graduate scholarships.

Conflicts of interest

There are no conflicts to declare.

Notes and references

1 X. Du, G. Wu and J. Cheng, *et al.*, *RSC Adv.*, 2017, **7**(17), 10391–10396.
2 Y. Dong, Y. Zou and J. Song, *et al.*, *J. Mater. Chem. C*, 2017, **5**, 11369–11394.
3 Y. He, M. Petryk and Z. Liu, *et al.*, *Nat. Photonics*, 2021, **15**, 36–42.
4 Y.-F. Xu, M.-Z. Yang and B.-X. Chen, *et al.*, *J. Am. Chem. Soc.*, 2017, **139**(16), 5660–5663.
5 A. Dey, J. Ye and A. De, *et al.*, *ACS Nano*, 2021, **15**(7), 10775–10981.
6 E. V. Ushakova, S. A. Cherevkov and A. V. Sokolova, *et al.*, *ChemNanoMat*, 2020, **6**(7), 1080–1085.
7 L. Protesescu, S. Yakunin and M. I. Bodnarchuk, *et al.*, *Nano Lett.*, 2015, **15**(6), 3692–3696.
8 B. Chen, P. N. Rudd and S. Yang, *et al.*, *Chem. Soc. Rev.*, 2019, **48**(14), 3842–3867.
9 M. Chen, J. Wang and F. Yin, *et al.*, *J. Mater. Chem. A*, 2021, **9**(8), 4505–4527.
10 Z. Wang, R. Li and Y. Zhang, *et al.*, *Adv. Mater.*, 2022, 2207923.
11 D. Nepal, S. Kang and K. M. Adstedt, *et al.*, *Nat. Mater.*, 2023, **22**, 18–35.
12 K. E. Shopsowitz, H. Qi and W. Y. Hamad, *et al.*, *Nature*, 2010, **468**, 422–425.
13 K. E. Shopsowitz, H. Qi and W. Y. Hamad, *et al.*, *J. Am. Chem. Soc.*, 2012, **134**(2), 867–870.
14 J. Zhang, Z. Meng and J. Liu, *et al.*, *ACS Appl. Mater. Interfaces*, 2019, **11**(45), 42629–42634.
15 M. Li, X. Lai and C. Li, *et al.*, *Mater. Today Nano*, 2019, **6**, 100039.
16 Y. Zhao, L. Shang and Y. Cheng, *et al.*, *Acc. Chem. Res.*, 2014, **47**(12), 3632–3642.
17 S. V. Vignolini, P. J. Rudall and A. V. Rowland, *et al.*, *PNAS*, 2012, **109**(39), 15712–15715.
18 K. Chen, S. Schünemann and H. Tüysüz, *Angew. Chem., Int. Ed.*, 2017, **56**, 6548.
19 M. Curti, J. Schneider and D. W. Bahnemann, *et al.*, *J. Phys. Chem.*, 2015, **6**(19), 3903–3910.
20 G. Collins, A. Lonergan and D. McNulty, *et al.*, *Adv. Mater. Interfaces*, 2020, **7**, 1901805.
21 G. L. Chiarello, A. Zuliani and D. Ceresoli, *et al.*, *ACS Catal.*, 2016, **6**(2), 1345–1353.
22 Q. Yang, M. Li and J. Liu, *et al.*, *J. Mater. Chem. A*, 2013, **1**, 541–547.
23 Y. Hou, S. Yuan and G. Zhu, *et al.*, *Adv. Mater.*, 2023, **35**, 2209004.
24 E. C. Nelson, N. Dias and K. Bassett, *et al.*, *Nat. Mater.*, 2011, **10**, 676–681.
25 Y. Li, M. E. Calvo and H. Míguez, *Adv. Opt. Mater.*, 2016, **4**, 464–471.
26 J. Wang, P. W. H. Pinkse and L. I. Segerink, *et al.*, *ACS Nano*, 2021, **15**(6), 9299–9327.
27 X. Zheng, Y. Hou and H. Sun, *et al.*, *J. Phys. Chem. Lett.*, 2019, **10**(10), 2629–2640.
28 S. Bera, R. K. Behera and S. D. Adhikari, *et al.*, *J. Phys. Chem.*, 2021, **12**(49), 11824–11833.
29 E. M. Purcell, H. C. Torrey and R. V. Pound, *PROLA*, 1946, **69**(1–2), 37–38.
30 S. Nishimura, N. Abrams and B. A. Lewis, *et al.*, *J. Am. Chem. Soc.*, 2003, **125**(20), 6306–6310.
31 R. Ahumada-Lazo, J. A. Alanis and P. Parkinson, *et al.*, *J. Phys. Chem. C*, 2019, **123**(4), 2651–2657.